

MONTE CARLO SIMULATION OF 3D SURFACE MORPHOLOGIES FOR SECONDARY ELECTRON EMISSION REDUCTION*

Q. Gibaru^{1†}, C. Inguibert, M. Belhaj, ONERA, Toulouse, France
M. Raine, D. Lambert, CEA/DAM, Arpajon, France
¹also at CEA/DAM, Arpajon, France and CNES, Toulouse, France

Abstract

Low energy electrons of few tens of eV may cause Multipactor breakdowns in waveguides driven by the Secondary Electron Emission Yield (SEY) of the walls. This risk is lowered by using low emissive surfaces and this topic has been studied experimentally and with numerical simulations. The dependence of the SEY on surface properties is well known. Surface morphology has been widely used to reduce the SEY by forming roughness patterns on the surface. All patterns do not have the same efficiency so their analysis in term of SEY is relevant. Monte-Carlo simulation codes can be used to study the processes behind the SEY. The MicroElec module of GEANT4 has recently been extended with more materials and processes, and validated with experimental data for SEY calculations. In this work, simulation results are shown for a bulk sample capped with different roughness patterns. The effects of the shape parameters on the SEY are studied for typical dimensions between 20 μm and 100 μm . The results are checked with experimental SEY measurements on samples with similar roughness patterns.

INTRODUCTION

Many devices, including satellite radio-frequency components (such as microwave wave guides) [1], fusion reactors and particle accelerators [2], operate under RF electric fields which can have an influence on the charged particles inside the device. In particular, low energy electrons between a few tens and a few hundred of eVs may cause an electronic avalanche enabled by the ambient RF field, which is also known as the Multipactor effect. The threshold for the Multipactor effect heavily depends on the secondary electron emission yield (SEY) of the walls of the device [3]. Indeed, if the SEY is greater than 1, the number of electrons extracted from the walls of the device is greater than the number of incident electrons, which can lead to the buildup of an electron cloud in the device. If the formation of the electron clouds is synchronized with the electric field frequency, a resonance phenomenon may amplify the production of electron clouds, which can lead to the Multipactor discharge. These discharges can disrupt the transmitted signal, and in extreme cases the walls can get physically damaged.

Consequently, to prevent the formation of electron clouds and the Multipactor effect, the SEY of the walls of the device should be as low as possible. However, many

materials used in space applications generally have a SEY greater than 1 for incident energies between 100 eV and 1 to 2 keV. These incident electrons have such energies that their penetration range is of the order of some nanometers [4]. Moreover, the secondary electrons escaping from the material are generally considered to have energies below 50 eV. As a result, the SEY is heavily dependent on the surface state of the material, such as surface contamination or roughness.

In many fields, materials with a specific surface state or roughness are developed to mitigate the SEY effects. A widely used option is to engineer a specific surface roughness pattern which can trap the secondary electrons emitted by the surface [5-11]. Indeed, the electrons emitted from the bottom of the roughness asperities may hit the side walls and get recollected, thus reducing the SEY. However, the presence of roughness may induce an opposing effect, as the incidence angle of the primary beam can get significantly increased if they hit the side walls of the roughness patterns for instance. Some authors have proposed different means of creating specific roughness patterns, for instance chemically or by laser engraving. The work shown in this paper is in line with this approach. We propose to study the influence of multiple roughness patterns on the SEY in the region of interest for multipactor ($\text{SEY} > 1$) by the use of a 3D Monte-Carlo simulation [12]. A validation is proposed by comparing the Monte-Carlo simulation and experimental data obtained on similar roughness patterns.

MONTE CARLO CODE FOR SEY SIMULATION

The simulation of the SEY of materials under electron irradiation is heavily dependent on the transportation of low energy electrons through and out of the target material. Indeed, the condition of occurrence of the multipactor discharge ($\text{SEY} > 1$) is generally met for electrons between 100 eV and 1 keV depending on the material. Moreover, most secondary electrons generated inside the material by the primary beam have energies of a few tens of eVs. The crossing of the surface by these very low energy electrons needs to be accurately modeled in order to not over-estimate the emission rate. Finally, the interactions with weakly bound electrons and plasmons need to be taken into account in particular, as these will be the main source of secondary electrons and induce energy losses of a couple tens of eVs. Consequently, a very precise description of the transportation of low energy electrons is needed to get accurate SEY computations from Monte-Carlo simulations.

* Work supported by ONERA, CEA/DAM and the French Space agency (CNES).

† quentin.gibaru@onera.fr

We have developed for some years the Monte-Carlo simulation tool MicroElec [12-15], focused on the transportation of low energy electrons for microdosimetry and SEY applications, under electron, proton and heavy ion irradiation. The latest developments of the MicroElec module are expected to be available in the June 2021 version of the GEANT4 toolkit for radiation-matter interaction simulation. In MicroElec, the inelastic interaction is modeled by the dielectric function theory, and the elastic interaction by the partial wave method. In particular, the simulation of low energy electrons in MicroElec has been validated with experimental SEY data. The SEY can thus be computed for 13 materials, including 11 monoatomic materials (C, Be, Al, Si, Ti, Ni, Fe, Cu, Ge, Ag, W) and 2 insulators (Kapton and SiO₂). All details can be found in refs [12-15].

In this work, MicroElec has been used to compute the SEY under electron irradiation, for incident energies between 0 and 2 keV on a semi-infinite silver sample capped with different roughness patterns. 10000 electrons with a normal incidence are simulated for each energy.

EFFECT OF ROUGHNESS PATTERNS ON THE SEY

Several roughness patterns can be used to reduce the SEY, such as rectangular and triangular grooves [5, 11], rectangular or trapezoidal checkerboard patterns [7, 8], or sawtooth grooves [6]. The presence of these patterns on a surface will limit the propagation of the secondary electrons emitted from the bottom of the structures, as the electrons can hit the side walls and penetrate in the material. The TEEY can thus be reduced by purely geometrical effects, which means that the relative reduction of the TEEY for a specific pattern of roughness can be expected to be similar for different materials. We can consequently compare the efficiency of different patterns on a single material and see which patterns produce the most beneficiary effects.

Previous simulations with our Monte-Carlo code [8] showed that rectangular grooved patterns were less efficient regarding SEY reduction. This is to be expected since rectangular grooves only limit the propagation of secondary electrons in one direction, whereas checkerboard patterns include cavities analogous to a porous surface, which can trap the secondary electrons. Triangular grooves may also be more efficient than rectangular grooves, as the valleys between the structures may be narrower. This work focuses on sawtooth and checkerboard patterns, made of regularly spaced rectangular and trapezoidal structures. These can be described using the parameters found on Figs. 1 and 2.

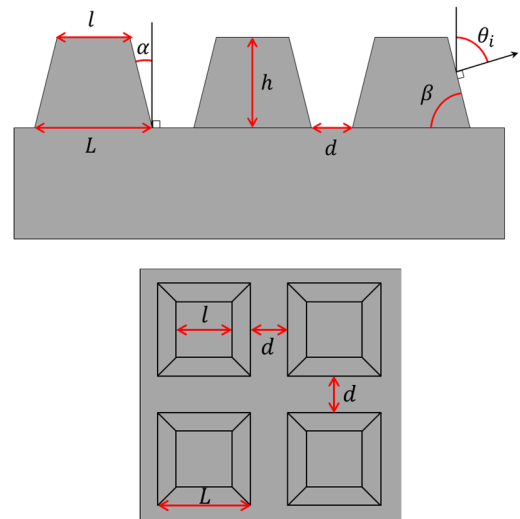


Figure 1: 2D Side view and top view of a trapezoidal checkerboard pattern.

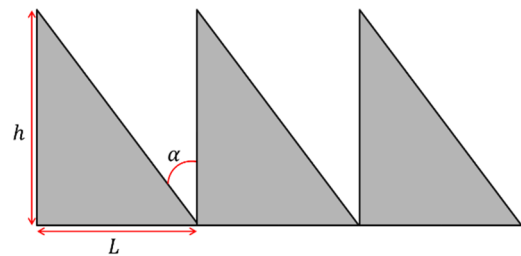


Figure 2: 2D Side view of a sawtooth groove pattern.

A checkerboard pattern is characterized by its base length L , upper length l , height h , the inter-structure distance d between two mounts, the openness of the recollection valleys α , and the periodicity $L+d$. In the case of a rectangular checkerboard, $L = l$ and $\alpha = 0^\circ$. The sawtooth pattern is also characterized by its base length L , height h and openness α .

Figure 3 shows simulation results of the reduction of the TEEY of silver induced by sawtooth grooves, and rectangular and trapezoidal checkerboard patterns of the same height ($h = 100 \mu\text{m}$) and base length ($L = 80 \mu\text{m}$). The trapezoidal checkerboards have an upper base length of $l = 40 \mu\text{m}$, their efficiency depends on the inter-structure distance. With no inter-structure distance, as in the case of the sawtooth pattern, the trapezoidal checkerboard (a) is the most effective and more efficient than the rectangular checkerboard and sawtooth grooves. However, for the trapezoidal checkerboard (b) with the same inter-structure distance as the rectangular checkerboard ($d = 80 \mu\text{m}$), the latter is more efficient. Indeed, at equal inter-structure distances, the straight walls provide better recollection as there are no tilted surfaces with a high incidence angle.

Content from this work may be used under the terms of the CC BY 3.0 licence (© 2021). Any distribution of this work must maintain attribution to the author(s), title of the work, publisher, and DOI

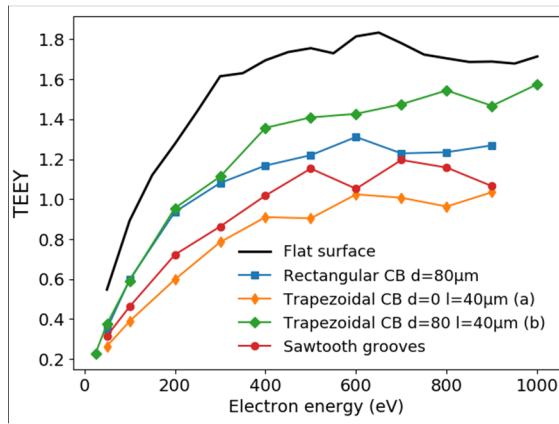


Figure 3: Comparison of roughness patterns with height = 100 μm and base length L = 80 μm.

The sawtooth pattern's efficiency is in between the two checkerboard patterns, and provides less TEEY reduction than the trapezoidal checkerboard (a). Indeed, for equal base lengths, the openness angle α of the recollection valleys will be smaller for the trapezoidal checkerboard than for the sawtooth pattern, which means better recollection. To get an equivalent α for the triangular grooves and sawtooth patterns, their base length and periodicity has to be reduced compared to the trapezoidal checkerboard, which increases TEEY reduction, as seen on Fig. 4.

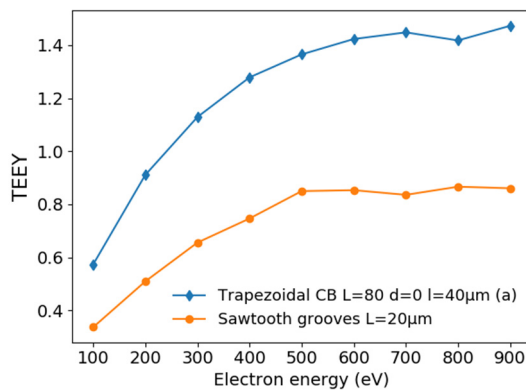


Figure 4: Comparison of roughness patterns with equal openness, height = 60 μm, no inter-structure distance.

Taller structures have also already been shown to be more efficient. Consequently, the periodicity, openness angle and height of the structures are the main parameters which can modify the resulting TEEY of the roughness pattern.

COMPARISON WITH EXPERIMENTAL DATA

Three samples of a checkerboard structured surface of Ag with structure heights of 20, 40 and 60 μm have been irradiated in the DEESSE facility at ONERA [1, 16] by a normal incidence electron beam. These samples can be used as a validation for our simulations. These can be compared to simulations of trapezoidal checkerboard patterns, with simulated dimensions of $L = 50 \mu\text{m}$, $l = 20 \mu\text{m}$, $d = 30 \mu\text{m}$ and $h = 20, 40$ and $60 \mu\text{m}$, as shown on Fig. 5.

Due to surface contamination on each experimental sample, a scale factor between 1.5 and 1.7 has to be applied to each simulated TEEY. In this case, the experimental and simulated SEYs are in satisfying agreement as they follow a similar evolution according to the structures' heights. We can consider that the Monte-Carlo code is able to faithfully simulate the recollection of secondary electrons due to geometrical effects.

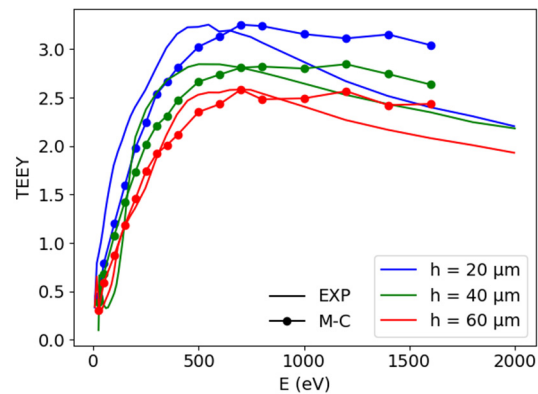


Figure 5: Comparison between experimental data (EXP) and simulated (M-C) TEEYs.

Although the work shown here focuses on the comparison between different roughness patterns using similar dimensions, each type of pattern may have a different efficiency depending on the dimensions used. Indeed, as mentioned in the introduction, two opposing effects can happen in the case of rough surfaces. The recollection effect induced by the valleys has been the focus of this work, but other dimensions with smaller heights and pointier structures may be used to increase the SEY by increasing the mean incidence angle of the electrons on the surface. Indeed, in the aforementioned example, the electrons are more susceptible to hit a tilted side wall with a high incidence angle, inducing a higher SEY. Consequently, the present work has been extended with a more in depth study of the influence of each geometrical parameter, which should be published in the near future.

REFERENCES

- [1] N. Balcon, D. Payan, M. Belhaj, T. Tondu, and V. Inguibert, "Secondary Electron Emission on Space Materials: Evaluation of the Total Secondary Electron Yield From Surface Potential Measurements", *IEEE Trans. Plasma Sci.*, vol. 40, no. 2, p. 282-290, Feb. 2012. doi:10.1109/TPS.2011.2172636
- [2] K. Ohmi, "Beam-Photoelectron Interactions in Positron Storage Rings", *Phys. Rev. Lett.*, vol. 75, n° 8, p. 1526-1529, Aug. 1995. doi:10.1103/PhysRevLett.75.1526
- [3] N. Fil, M. Belhaj, J. Hillairet, and J. Puech, "Multipactor threshold sensitivity to Total Electron Emission Yield in parallel-plate waveguide and TEEY models accuracy", in *2016 IEEE MTT-S International Microwave Symposium (IMS)*, May 2016, p. 16213647, p. 1-4. doi:10.1109/MWSYM.2016.7540278
- [4] C. Inguibert, M. B. Belhaj, D. Lambert, M. Raine, and Q. Gibaru, "Extrapolated Range for Low Energy Electrons (< 1 keV)", presented at the 12th Int. Particle Accelerator Conf. (IPAC'21), Campinas, Brazil, May 2021, paper THPAB210, this conference.
- [5] M. Pivi, F. K. King, R. E. Kirby, T. O. Raubenheimer, G. Stupakov, and F. Le Pimpec, "Sharp reduction of the secondary electron emission yield from grooved surfaces", *J. Appl. Phys.*, vol. 104, no. 10, p. 104904, Nov. 2008. doi:10.1063/1.3021149
- [6] L. Wang, T. O. Raubenheimer, and G. Stupakov, "Suppression of secondary emission in a magnetic field using triangular and rectangular surfaces", *Nucl. Instrum. Methods Phys. Res., Sect. A*, vol. 571, no. 3, p. 588-598, Feb. 2007. doi:10.1016/j.nima.2006.11.039
- [7] R. Valizadeh, O. B. Malyshev, S. Wang, S. A. Zolotovskaya, W. A. Gillespie, and A. Abdolvand, "Low secondary electron yield engineered surface for electron cloud mitigation", *Appl. Phys. Lett.*, vol. 105, no. 23, p. 231605, Dec. 2014. doi:10.1063/1.4902993
- [8] J. Pierron, C. Inguibert, M. Belhaj, J. Puech, and M. Raine, "Effect of rectangular grooves and checkerboard patterns on the electron emission yield", *J. Appl. Phys.*, vol. 124, no. 9, p. 095101, Sept. 2018. doi:10.1063/1.5028216
- [9] J. M. Sattler, R. A. Coutu, R. Lake, T. Laurvick, T. Back, and S. Fairchild, "Modeling micro-porous surfaces for secondary electron emission control to suppress multipactor", *Journal of Applied Physics*, vol. 122, no. 5, p. 055304, Aug. 2017. doi:10.1063/1.4997465
- [10] L. Aguilera *et al.*, "CuO nanowires for inhibiting secondary electron emission", *J. Phys. D: Appl. Phys.*, vol. 46, no. 16, p. 165104, Mar. 2013. doi:10.1088/0022-3727/46/16/165104
- [11] K. Nishimura, T. Itotani, and K. Ohya, "Influence of Surface Roughness on Secondary Electron Emission and Electron Backscattering from Metal Surface", *Jpn. J. Appl. Phys.*, vol. 33, no. 8R, p. 4727, Aug. 1994. doi:10.1143/JJAP.33.4727
- [12] Q. Gibaru, C. Inguibert, P. Caron, M. Raine, D. Lambert, and J. Puech, "Geant4 physics processes for microdosimetry and secondary electron emission simulation: Extension of MicroElec to very low energies and 11 materials (C, Al, Si, Ti, Ni, Cu, Ge, Ag, W, Kapton and SiO₂)", *Nuclear Instruments and Methods in Physics Research Section B: Beam Interactions with Materials and Atoms*, vol. 487, p. 66-77, Jan. 2021. doi:10.1016/j.nimb.2020.11.016
- [13] A. Valentin, M. Raine, J. -E. Sauvestre, M. Gaillardin, and P. Paillet, "Geant4 physics processes for microdosimetry simulation: Very low energy electromagnetic models for electrons in silicon", *Nucl. Instrum. Methods Phys. Res., Sect. B*, vol. 288, p. 66-73, Oct. 2012. doi:10.1016/j.nimb.2012.07.028
- [14] A. Valentin, M. Raine, M. Gaillardin, and P. Paillet, "Geant4 physics processes for microdosimetry simulation: Very low energy electromagnetic models for protons and heavy ions in silicon", *Nucl. Instrum. Methods Phys. Res., Sect. B*, vol. 287, p. 124-129, Sept. 2012. doi:10.1016/j.nimb.2012.06.007
- [15] M. Raine, M. Gaillardin, and P. Paillet, "Geant4 physics processes for silicon microdosimetry simulation: Improvements and extension of the energy-range validity up to 10 GeV/nucleon", *Nucl. Instrum. Methods Phys. Res., Sect. B*, vol. 325, p. 97-100, Apr. 2014. doi:10.1016/j.nimb.2014.01.014
- [16] T. Gineste, M. Belhaj, G. Teyssedre, and J. Puech, "Investigation of the electron emission properties of silver: From exposed to ambient atmosphere Ag surface to ion-cleaned Ag surface", *Appl. Surf. Sci.*, vol. 359, p. 398-404, Dec. 2015. doi:10.1016/j.apsusc.2015.10.121